International Journal of Nanomedicine

Dovepress
open access to scientific and medical research

Open Access Full Text Article

ORIGINAL RESEARCH

Repeated intravenous administration of silica nanoparticles induces pulmonary inflammation and collagen accumulation via JAK2/STAT3 and TGF-β/Smad3 pathways in vivo

This article was published in the following Dove Press journal:
International Journal of Nanomedicine

Yang Yu[1,2]
Tingting Zhu[1]
Yang Li[1,2]
Li Jing[1,2]
Man Yang[1,2]
Yanbo Li[1,2]
Junchao Duan[1,2]
Zhiwei Sun[1,2]

[1]Department of Toxicology and Sanitary Chemistry, School of Public Health, Capital Medical University, Beijing, People's Republic of China; [2]Beijing Key Laboratory of Environmental Toxicology, Capital Medical University, Beijing, People's Republic of China

Background: The health hazards of silica nanoparticle (SiNP) are raising worldwide concern as SiNPs has become the second largest manufactured nanomaterial in global markets. However, insufficient data for the adverse health effects and safety evaluation of SiNPs are remaining a big question.

Purpose: We evaluated the effects and related mechanism of SiNPs on pulmonary inflammation and collagen production through repeated intravenous administration in mice in a 45-day observation period.

Methods: Morphological and ultrastructural change, ultradistribution of SiNPs in lungs were observed in ICR mice through intravenous administration. Oxidative damage, pro-inflammatory cytokines, hydroxyproline content, the marker of fibroblasts and epithelial-mesenchymal transition (EMT), and JAK2/STAT3 and TGF-β1/Smad3 signaling pathways were detected to explore the lung injuries and related mechanism.

Results: The results showed repeated intravenous exposure of SiNPs increased the weight of lung tissues and destroyed pulmonary histomorphological structure. The increased MDA content, depletion of SOD and GSH-Px in lungs were observed in SiNP-treated mice. The protein expressions of JAK2/STAT3 pathway were upregulated in lungs, and the levels of inflammatory cytokines TNF-α, IL-1β, and IL-6 in serum and lungs were also elevated in SiNPs treated group. The increased hydroxyproline content indicated collagen accumulation in lungs of SiNP-treated mice. Meanwhile, the protein expressions of the marker of myofibroblast (a-SMA), the regulators in connective tissue remodeling (CTGF), TGF-β, and p-Smad3 were all upregulated in lungs. In addition, we found intravenous administration of SiNPs-induced ultrastructural changes in type II alveolar epithelial cells but without downregulation of the protein expression of the key markers of epithelial cells (E-Cadherin).

Conclusion: Our results revealed that oxidative stress and inflammation contributed to the collagen accumulation through activation of JAK2/STAT3 and TGF-β/Smad3 pathways. It suggests that pulmonary aberrant inflammation and collagen accumulation induced by nanoparticles should be seriously considered for the safety application in diagnostics or therapeutics.

Keywords: Silica nanoparticles, repeated intravenous administration, inflammation, collagen accumulation, JAK2/STAT3 signaling pathway, TGF-β/Smad3 signaling pathway

Correspondence: Zhiwei Sun; Junchao Duan
Department of Toxicology and Sanitary Chemistry, School of Public Health, Capital Medical University, Beijing 100069, People's Republic of China
Tel +86 01 08 391 1507;
+86 01 08 391 1868
Email zwsun@ccmu.edu.cn;
jcduan@ccmu.edu.cn

Introduction

Nanotechnology environmental health and safety, normally known as NanoEHS, is a new emerged research discipline on nanotoxicity which warrants global rigorous attention on the hazard and risk potential of manufactured nanomaterials.[1] Silica

nanoparticles (SiNPs) have the nano-scaled size and the unique physicochemical properties such as higher surface reactivity and increased surface-to-volume ratio.[2,3] Due to the appealing properties of SiNPs, they have been widely applied in the areas of coating, cosmetics, and food.[4] The 2017 World Health Organization (WHO) guidelines indicated the annual production volume of SiNPs was 1.5 million tonnes, suggesting SiNPs have been the second largest manufactured nanomaterial in global markets.[5] In this regards, the hazard risks of population exposure and environmental exposure to SiNPs have been raised. Furthermore, with the high biocompatibility and stability, SiNPs are the perfect candidate in the biomedical application of imaging, drug delivery, and gene therapy, in which SiNPs could enter the human body directly.[4,6] Due to the large-scale production of SiNPs and increased potential of SiNPs exposure, it is necessary to pay attention to the health hazard and safety evaluation of SiNPs. Although US Food and Drug Administration (FDA) permitted a cancer-targeted probe of SiNPs for Stage I clinical trials as early as 2011,[7] there is still insufficient or lack of data available for the adverse health effects of SiNPs.[8]

In the biomedical application such as disease diagnosis or gene therapy, intravenous injection is the usual route of SiNPs exposure. The reticuloendothelial system, especially in liver, is thought to be the main target organ and it was reported that intravenous injection of SiNPs could induce liver granuloma and fibrosis in vivo.[9] A few researches reported that the lung is one of the first three organs that SiNPs mainly accumulated in after intravenous injection.[10,11] Our previous study found that intravenous injection of SiNPs induced CD68-positive macrophages infiltration in mice lungs in an acute toxicity study.[10] Serge et al found that intravenous injection of SiNPs induced mast cells accumulation in lungs and increased collagen fibers in the alveolar septa, but they did not further explore the related signal pathways involved in this process.[12] Recently, Raziye reported that SiNPs caused lung thrombosis and inflammation through intravenous injection in vivo.[13] But the later scenarios, more details and related mechanisms need further exploration.

This study was aimed to assess the pulmonary toxicity of SiNPs and further investigate the related mechanism through repeated intravenously administration in mice. Morphological changes, ultrastructural changes, and ultradistribution of SiNPs in lungs were observed. Oxidative damage was used to assess lung injury. Pro-inflammatory cytokines in the serum and lungs were detected to assess the systemic and pulmonary inflammation. The collagenous fiber content, the marker of fibroblasts, and epithelial–mesenchymal transition (EMT) were tested to evaluate collagen accumulation. The activation of JAK2/STAT3 and TGF-β1/Smad3 signaling pathways was detected to confirm whether these two pathways had participated in the progress of inflammation or collagen accumulation in lungs induced by SiNPs. Moreover, the subacute and chronic pulmonary injuries after intravenous administration of SiNPs with three time points were set in this study. It will provide a comprehensive understanding and valuable evidence for the safety evaluation and the biomedical application of SiNPs in diagnostics or therapeutics.

Materials and methods

SiNPs preparation and characterization

The SiNPs were prepared as previously described.[10] The shape and size of SiNPs were observed by transmission electron microscope (TEM, JEM2100, Japan). The Zeta potential and hydrodynamic sizes of SiNPs in dispersion media were determined by Zeta electric potential granulometer (Malvern Nano-ZS90, UK). The content of endotoxin in SiNPs was analyzed using Gel clot Limulus Amebocyte Lysate (LAL) assay.

Animals and experimental design

ICR mice (weight 20–22 g, 8 weeks old, male) were obtained from Vital River Laboratory Animal Technology Company (Beijing, China). Prior to the final treatment, the mice were kept fasted overnight. All the animal experiments were approved by the Committee of Laboratory Animal Care and Use in Capital Medical University, and all the procedures followed the National Guidelines for Animal Care and Use. The dosage of repeated intravenous administration of SiNPs was 20 mg/kg body weight, which was based on our previous study on the acute toxicity of SiNPs. The mice were intravenously administrated with SiNPs at 20 mg/kg body weight repeatedly, once per three days, five times totally. The mice in control groups were injected with the same volume of saline intravenously. The animal mortality and clinical manifestation in each group were recorded. The mice were sacrificed at 15th day, 30th day, and 60th day after first injection, and the blood and the lungs were harvested. The experimental design is shown in Figure S1.

Histopathology

The lungs were fixed in 10% formalin for 24 hrs, and then were embedded in paraffin. Four-millimeter sections were

deparaffinized and stained with hematoxylin and eosin. Then, the histopathology examination was conducted using the optical microscope (X71-F22PH, Olympus, Japan). The pathologist was completely blinded to the experiment design.

Ultrastructural observation by TEM

The fresh mice lungs were excised and immediately put in 2.5% glutaraldehyde. Then, the lungs were quickly cut into small pieces as 0.5 mm×0.5 mm. After fixation overnight, the lung samples were rinsed with 0.1 M PB and embedded in 2% agarose gel. Then, the samples were post-fixed in 4% osmium tetroxide. After being stained with 0.5% uranyl acetate and dehydrated in ethanol with concentration gradients, the lung samples were embedded in epoxy resin. The ultrathin sections (50 nm) were obtained and were observed using TEM.

Assessment of oxidative stress

The lung tissues (100 mg) were homogenized in saline on ice. The homogenates were then centrifuged at 3000 rpm, 4°C, for 10 mins. The supernatants were collected to measure the MDA content and the SOD and GSH-Px activities with commercially available kits (Nanjing Jiancheng, China). Meanwhile, the total protein concentration of the homogenates was detected using the kits of bicinchoninic acid (BCA) protein assay (Nanjing Jiancheng, China).

Determination of pulmonary hydroxyproline (HYP) content

The HYP content in lungs (100 mg) was measured through Kivirikko's method with some modification using HYP assay kits (Nanjing Jiancheng, China).[14] The HYP contents were expressed as milligrams of HYP per gram of wet lung weight.

Inflammatory cytokines measurement

Blood samples were collected via the ocular vein at 15th day, 30th day, and 60th day. The serum was obtained by centrifugation of the whole blood at 3000 rpm for 15 mins. The supernatants of lung tissues were prepared as mentioned in the section "Assessment of oxidative stress". The levels of mouse interleukin-1β (IL-1β), mouse interleukin-6 (IL-6), and mouse tumor necrosis factor-α (TNF-α) in serum and in the lungs were measured by ELISA kits (Lanbing, Dakewei, China) according to the manufacturer's protocols. Absorbance at 450nm was tested by a microplate reader (Thermo Multiskan™ MK3, USA). The total protein concentration of the lung homogenates was detected using BCA protein assay kits (Nanjing Jiancheng, China).

Immunohistochemical staining

The expression of α-Smooth Muscle Actin (αSMA), the marker of myofibroblast, and connective tissue growth factor (CTGF), the main regulators in connective tissue remodeling or fibrosis, was detected using immunohistochemical staining in the paraffin-embedded lung sections. After deparaffinating, rehydration, and antigen retrieval, the lung sections were treated with 3% H_2O_2 in order to quench endogenous peroxidase activity. Then, the sections were incubated with primary antibodies: αSMA [Cell Signaling Technology (CST), USA], CTGF (Abcam, USA), at 4°C overnight after blocking with 10% normal goat serum. The equivalent amount of normal goat IgG was added as a negative control. The sections were then stained with 3-3′ diaminobenzidine substrate and counterstained with hematoxylin following the standard procedure. All the analysis of the slides was blind to the pathologist. A brown staining indicates the positive expression. Then, the histopathology examination was conducted using the optical microscope. The pathologist was completely blinded to the experiment design.

Western blot analysis

Tissue Total Protein Extraction Kit (KeyGEN, China) was used to extract the total protein of lung tissue and the total protein concentration was determined by using the BCA protein kit. A total of 40 μg lysate proteins were loaded on SDS-polyacrylamide gels and transferred to nitrocellulose membranes (Pall 66,485, USA). Then, the membrane was blocked using fat-free milk at room temperature for 2 hrs and incubated at 4°C overnight. The primary antibodies E-cadherin, vimentin, and JAK2 were purchased from Cell Signaling Technology (CST), USA. The primary antibodies STAT3, p-STAT3, TGF-β, p-Smad3, and Smad3 were purchased from Abcam, USA. Finally, the photodensitometric analysis of the protein bands was conducted with the Image Lab™ Software (Bio-Rad, USA).

Statistical analysis

All the data were presented as mean±standard deviation (SD). A 2×2 factorial analysis was performed to determine the significance between groups. The statistical analysis was conducted using IBM SPSS Statistics version 21. Statistical difference was determined significantly at $P<0.05$.

Results

Characterization of SiNPs

The characterization of SiNPs was demonstrated in the supplemental material. The average size of the SiNPs was 62±7.1 nm (Figure S2), and the SiNPs had good monodispersability both in distilled water and saline (Table S1). The purity of the SiNPs was higher than 99.9% and no endotoxin was detected in the SiNPs by the LAL assay (Table S2).

Lung injuries induced by intravenous injection of SiNPs

The coefficients of lungs slightly elevated with time both in the SiNP-treated group and in the control group in the period of observation at three time points. The values in the SiNP-treated groups were significantly higher than that in the control groups at 15th day, 30th day, and 60th day (Figure 1A).

The lung sections of control groups revealed normal bronchial structure. In the SiNP-treated groups at 15th day, a large amount of red blood cells appeared in the area of alveoli induced indicating SiNPs induced severe congestion and hemorrhage of alveoli (Figure 1B d). At 30th day and 60th day, obvious alveoli septum thickening and inflammatory cell infiltration were observed in the lungs of the SiNP-treated mice (Figure 1B e and f).

Ultrastructural observation revealed that SiNPs were occasionally observed aggregated and enclosed with lysosome membranes in the cells of the lungs at 15th day (Figure 1C a and b). Alveolar macrophages

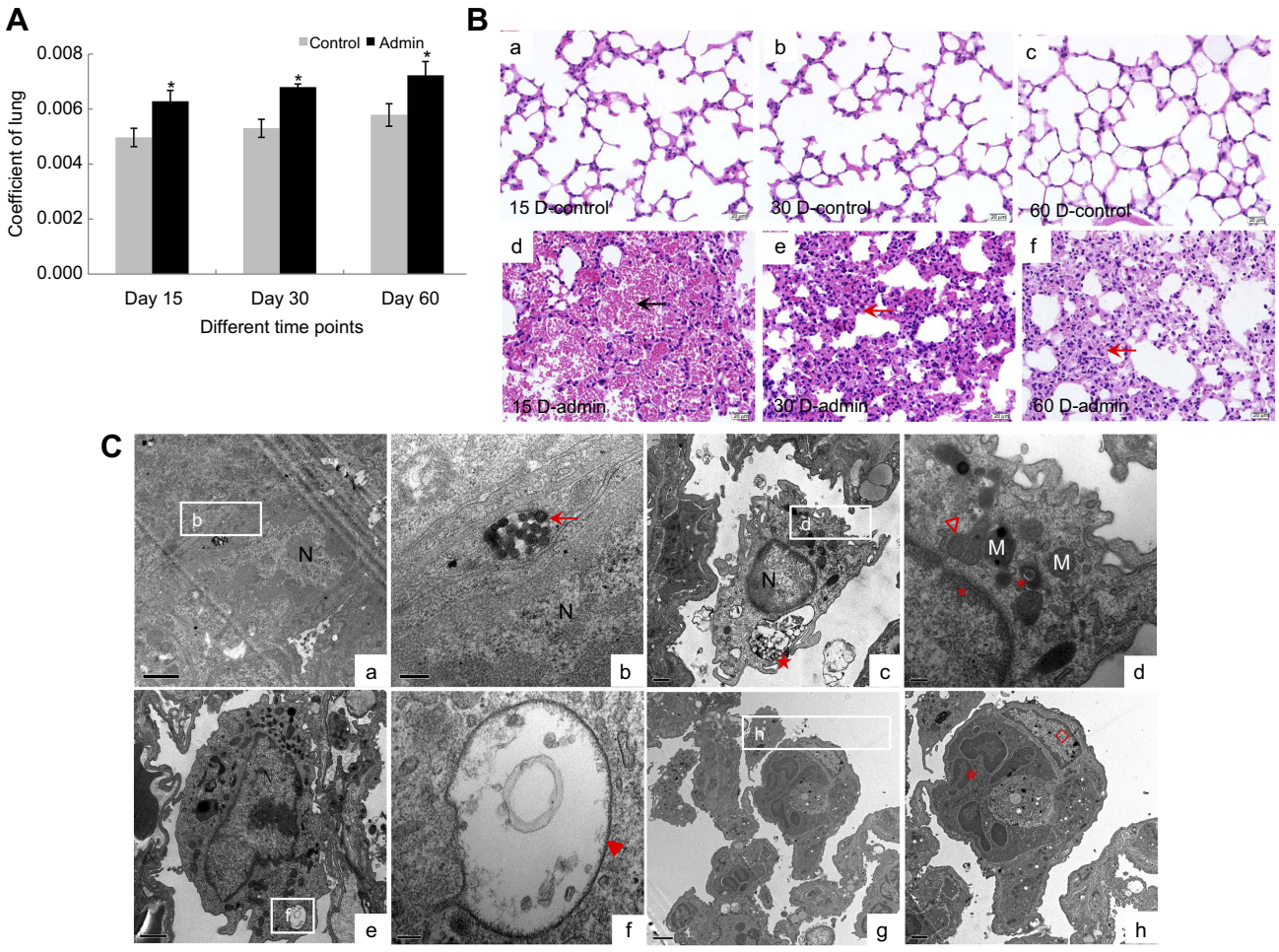

Figure 1 Lung injuries induced by SiNPs through intravenous injection in mice. (**A**) The coefficients of lungs increased significantly in the SiNP-treated group. Data are expressed as means±SD (n=5). *$P<0.05$ compared with control. (**B**) Histopathologic changes in mice lungs induced by SiNPs. Black arrow: red blood cells in the area of alveoli; Red arrow: alveoli septum thicken and inflammatory cell infiltration. Scale bar: 20 μm. (**C**) Ultrastructural observation in mice lungs observed by TEM. (a, b) SiNPs (red arrows) deposited in lungs at 15th day. Scale bar: (a) 1 μm; (b) 200 nm. (c, d) Ultrastructural changes of alveolar macrophages in lungs of SiNP-treated mice at 30th day: extensive vacuolization (red star), mitochondrial fusion (red hollow triangle), mitochondrial cristae disappearance (red asterisk). Scale bar: (c) 0.5 μm; (d) 200 nm. (e, f) Vacuolization (red triangle) in the basophilic granulocyte in lungs of SiNP-treated mice at 30th day. Scale bar: (e) 1 μm; (f) 100 nm. (g, h) Cell cluster consisted of multinucleate cell (hollow star) and type I alveolar epithelial cell (hollow diamond) in lungs of SiNP-treated mice at 60th day. Scale bar: (e) 2 μm; (f) 1 μm.

showed destruction of organelle such as mitochondrial fusion, mitochondrial cristae disappearance, and an extensive vacuolization in the SiNP-treated groups at 30th day (Figure 1C c and d). The vacuolization was also observed in the basophilic granulocyte in the lungs of SiNP-treated mice (Figure 1C e and f). At 60th day, the cell cluster appeared in the lungs in the administration group, which consisted of multinucleate cell and type Ⅰ alveolar epithelial cell (Figure 1C g and h).

Effects of SiNPs on the oxidative damage, inflammation, and JAK2/STAT3 signaling pathway in lungs

As shown in Figure 2A, the content of MDA, which is a product of lipid peroxidation, increased significantly in the lungs in the SiNP-treated mice compared with that in the control groups ($p<0.05$) at 15th day, 30th day, and 60th day and was 1.40-fold, 1.26-fold, and 1.16-fold higher than that in the control groups, respectively. On the contrary, the activities of SOD and GSH-Px which belong to the defense systems against free radical attack decreased at 15th day and 30th day in lungs in the SiNP-treated mice, and recovered and even elevated at 60th day. But only the changes of SOD activities in lungs in the SiNP-treated groups had significant statistical differences compared with control groups at three time points ($P<0.05$).

In order to assess the status of inflammation systemically and locally, we detected the pro-inflammatory cytokines in serum and in lungs. As shown in Figure 2B, SiNPs induced higher TNF-α, IL-1β, and IL-6 levels in lung tissues in experimental groups than in control groups at 15th day, at 30th day, and at 60th day. In SiNP-treated mice, TNF-α and IL-6 levels reached the peak value at 60th day while IL-1β levels at 15th day, which means IL-1β might be the most sensitive marker in local inflammation in lungs. Similarly, the serum TNF-α, IL-1β, and IL-6 levels were elevated significantly in SiNP-treated mice compared with that in control groups at 30th day and at 60th day (Figure 2C). Serum TNF-α level kept increasing while serum IL-1β and IL-6 decreased mildly in the whole observation period.

Figure 2D shows the protein expressions of key molecules in JAK2/STAT3 a pathway by Western blot. The densitometric analysis of the bands indicated the pulmonary expression of JAK2, p-STAT3, and STAT3 all increased significantly in SiNP-treated mice compared with that in control groups at three time points. The results turned out intravenous injection of SiNPs activated the JAK2/STAT3 pathways in lungs at 15th day, 30th day, and 60th day.

Effects of SiNPs on the myofibroblast activation, collagen production, and TGF-β/Smad3 signaling pathway in lungs

Figure 3A shows the expression of αSMA, the marker of myofibroblast by immunohistochemical staining in the lungs. Normally the expression of αSMA distributed in the vascular wall or the mesenchyme in lungs in control groups. In SiNP-treated mice, the number of αSMA positive cells increased in the pulmonary mesenchyme especially in pulmonary alveolar wall, and the αSMA positive cells always located in the area of inflammatory cells infiltration.

The immunohistochemistry of CTGF, which is one of the main regulators in connective tissue remodeling or fibrosis, is shown in Figure 3B. CTGF immunohistochemistry revealed more prominent pulmonary alveolar or interstitial CTGF staining in SiNP-treated mice than in control groups.

As the index of collagen accumulation, the hydroxyproline content was raised in lungs in the SiNP-treated mice with significant difference compared with control groups at three time points (Figure 3C). The changes of collagen content did not show obvious time tendency in the period of study, and SiNPs induced the pulmonary hydroxyproline contents elevated 1.07-, 1.16-, and 1.08-fold over control values at 15th day, 30th day, and 60th day, respectively.

The protein expressions of key molecules in TGF-β/Smad3 pathway by Western blot are shown in Figure 3D. The densitometric analysis of the bands indicated the pulmonary expression of TGF-β, p-Smad3, and Smad3 all increased significantly in SiNP-treated mice compared with that in control groups at three time points. The results illustrated intravenous injection of SiNPs activated TGF-β/Smad3 pathway in lungs at 15th day, 30th day, and 60th day.

Effects of SiNPs on the status of EMT in lungs

Intravenous administration of SiNPs induced ultrastructural changes in type II alveolar epithelial cells in lungs.

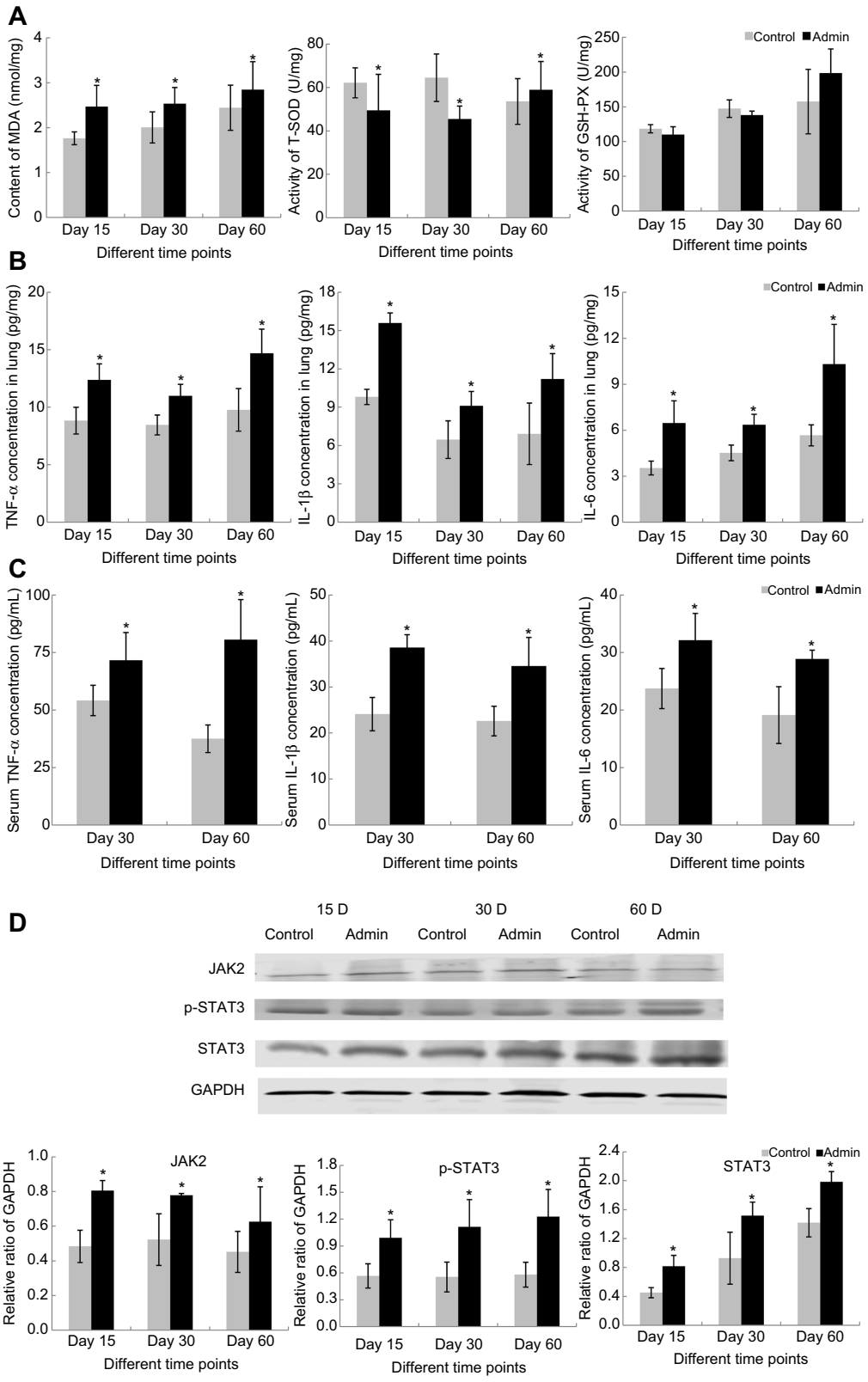

Figure 2 Effects of SiNPs on the oxidative damage, inflammation, and JAK2/STAT3 signaling pathway in lungs. (**A**) Effects of SiNPs on the oxidative damage in lung tissues. Data are expressed as means±SD (n=5). *P<0.05 compared with control. (**B**) Effects of SiNPs on the pro-inflammatory cytokines in lung tissues. Data are expressed as means±SD (n=5). *P<0.05 compared with control. (**C**) Effects of SiNPs on the pro-inflammatory cytokines in serum. Data are expressed as means±SD (n=5). *P<0.05 compared with control. (**D**) Western blot and relative densitometric analysis indicated SiNPs activated the JAK2/STAT3 signaling pathway in lung tissues at 15th day, 30th day, and 60th day. Data are expressed as means ± SD *P<0.05 compared with control.

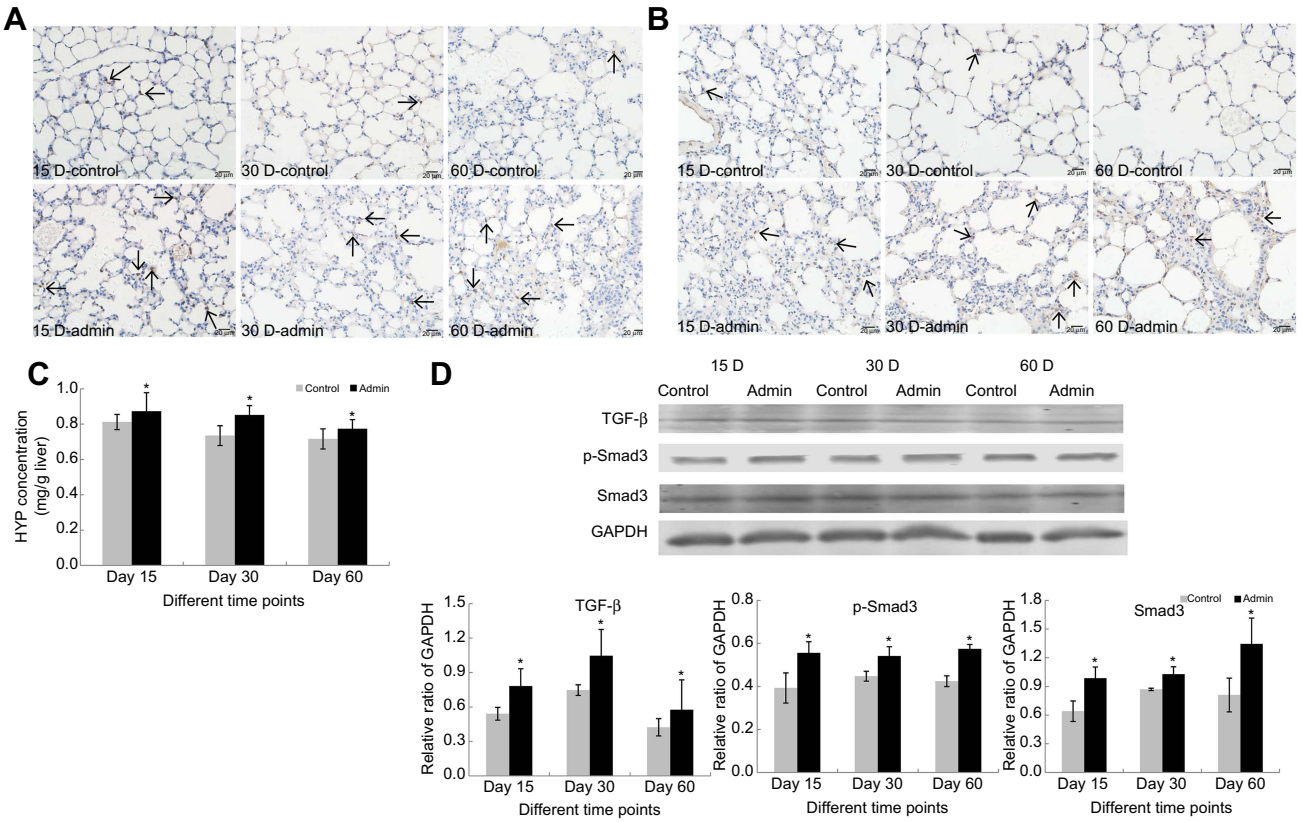

Figure 3 Effects of SiNPs on the myofibroblast activation, collagen production, and TGF-*P*/Smad3 signaling pathway in lungs. (**A**) Immunochemical staining of αSMA in lung sections. Black arrows: αSMA positive cells. Scale bar: 20 μm. (**B**) Immunochemical staining of CTGF in lung sections. Black arrows: CTGF positive cells. Scale bar: 20 μm. (**C**) The hydroxyproline level in lung tissues. Data are expressed as means±SD. **P*<0.05 compared with control. (**D**) Western blot and relative densitometric analysis indicated SiNPs activated the TGF-I3/Smad3 signaling pathway in lung tissues at 15th day, 30th day, and 60th day. Data are expressed as means±S.D. **P*<0.05 compared with control.

The type II alveolar epithelial cells in control groups appeared round shape and attached to the inner side of alveolar wall, with normal structure of nucleus, mitochondria, and lamellar body. In the SiNP-treated mice, the type II alveolar epithelial cells were viewed with irregular shape, nucleus irregularly shaped with folded membrane, lamellar bodies highly expansion, as well as collagenous fibers accumulation near the cell (Figure 4A).

The protein expression of E-cadherin, the key markers of epithelial cells, was significantly upregulated in lungs in the SiNP-treated mice compared with control groups at 15th day, 30th day, and 60th day, and appeared in a time-dependent manner (Figure 4B). Interestingly, SiNPs induced the protein expression of vimentin elevated at 15th day but decreased at 30th day and 60th day, without any statistical difference.

Thus, our data confirmed that intravenous injection of SiNPs induced pulmonary inflammation and collagen accumulation via JAK2/STAT3 and TGF-β/Smad3 pathways in vivo. A schematic model of the underlying mechanisms on how SiNPs regulate pulmonary injury is presented in Figure 5.

Discussion

As the rapid development of nanotechnology, concerns about the potential adverse biological outcome of manufactured nanomaterials are getting great attention. As one of the cornerstones of sustainability, the studies on NanoEHS to fill the large knowledge gaps in this field are required for the implementation and safe development of nanotechnology. For the first time, our study systemically evaluated the subchronic lung toxicity induced by repeated intravenous exposure of SiNPs in vivo. The results demonstrated that repeated intravenous injection of SiNPs could indeed cause pulmonary inflammation and collagen accumulation in vivo. It is helpful for the understanding of the organic toxicity through intravenous exposure of nanoparticles, so as to reduce the side effects in biomedical application of nanoparticles in diagnostics or therapeutics.

Most in vivo pulmonary toxicity studies of SiNPs chose intratracheal instillation exposure because it was the most common way for SiNPs exposure which mimicked the occupational exposure in human.[15–17] In intratracheal instillation exposure, SiNPs had direct

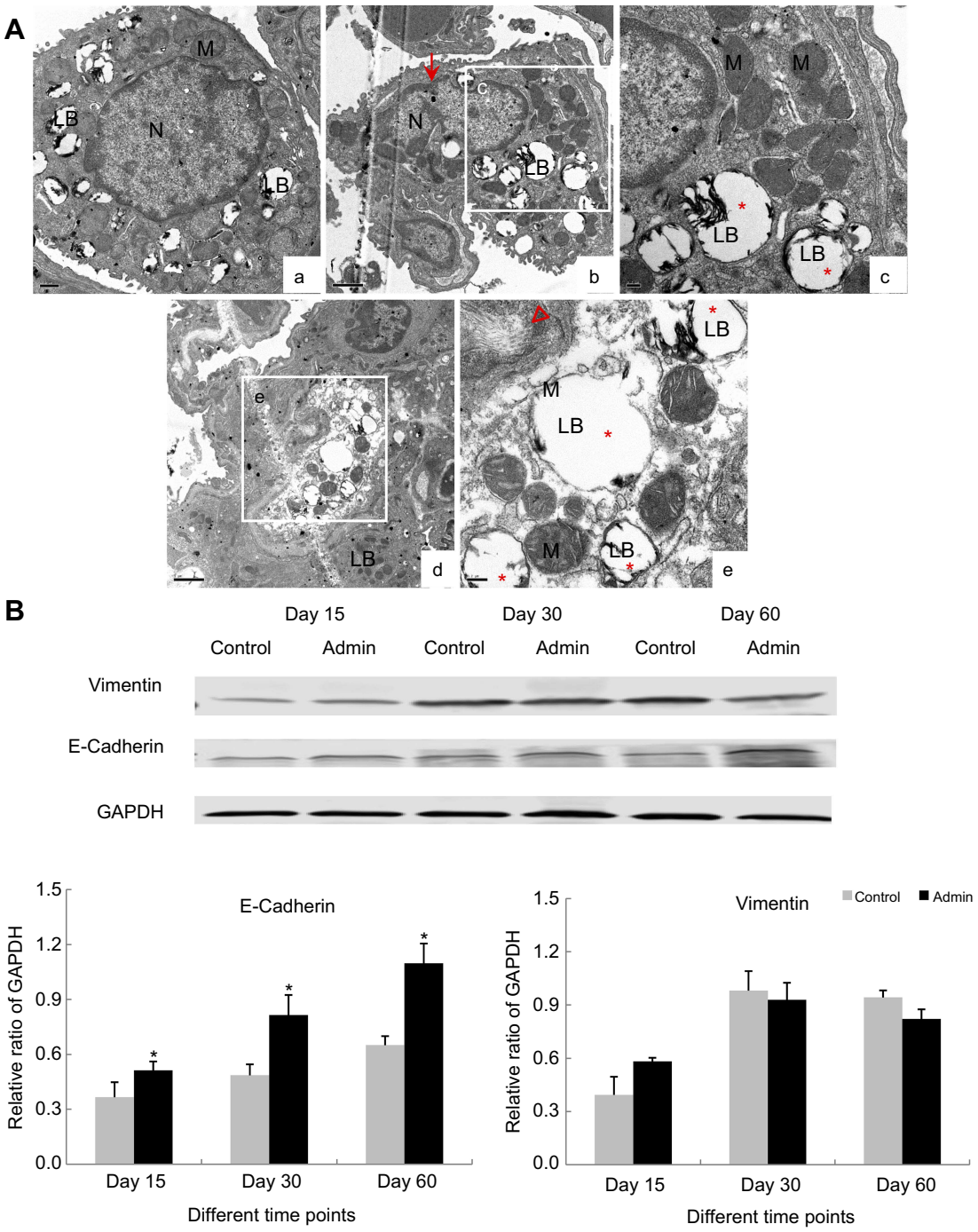

Figure 4 Effects of SiNPs on the status of epithelial–mesenchymal transition in lungs. (**A**) Ultrastructural changes of type II alveolar epithelial cells observed by TEM in mice lungs at 60th day. (a) Type II alveolar epithelial cell in the control group at 60th day. Scale bar: 0.5 μm; (b,c) Type II alveolar epithelial cell with irregular shape, nucleus transformation with fold membrane (red arrow), lamellar bodies expansion (red asterisk). Scale bar: 0.2 μm. (d, e) Type II alveolar epithelial cell with lamellar bodies highly expansion (red asterisk) and collagenous fibers accumulation nearby the cell (red hollow triangle). Scale bar: (d) 1 μm; (e) 0.2 μm. (**B**) Western blot and relative densitometric analysis of E-cadherin and vimentin in lungs at 15th day, 30th day, and 60th day. Data are expressed as means±S.D. *P<0.05 compared with control.

contact with the lung tissues and then deposited in situ, thus led to pulmonary injuries.[18–20] Ferri et al observed that systemic sclerosis patients with occupational exposure showed high serum levels of SiNPs, indicating SiNPs in the blood circulation acted as a co-factor involved in the etiopathogenesis of lung injuries.[21] In the present study, intravenous exposure of SiNPs increased the weight of lung tissues and destroyed pulmonary histomorphological structure and cellular ultrastructure (Figure 1). The results implied pulmonary injuries should be seriously taken into

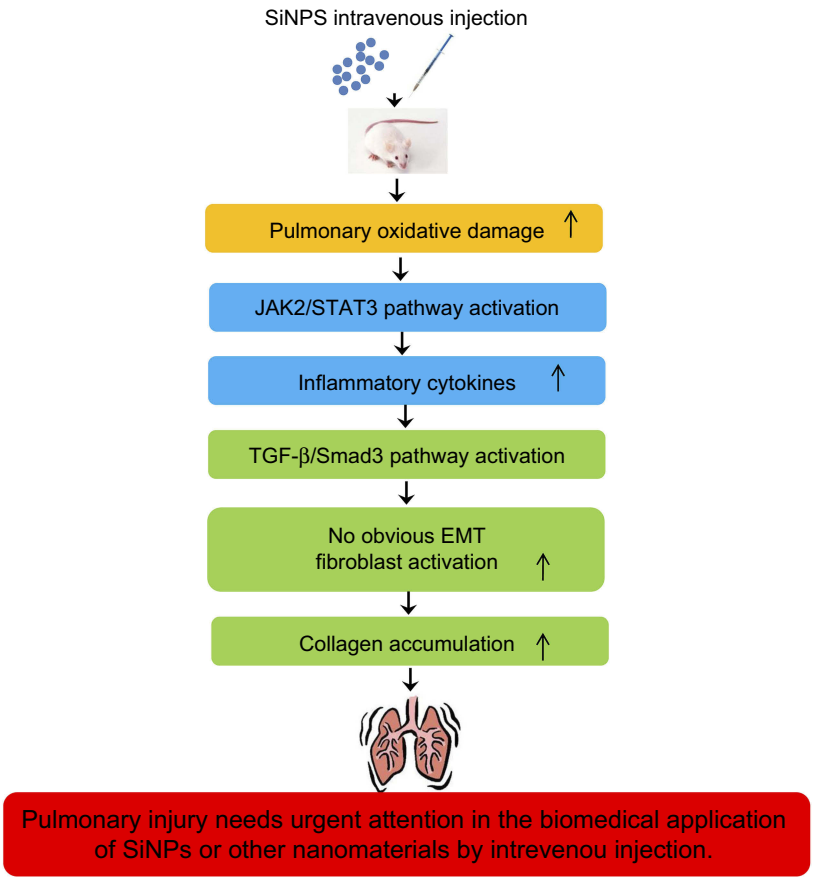

Figure 5 A schematic model on how SiNPs modulate pulmonary inflammation and collagen accumulation through repeated intravenous injection was presented. Briefly, SiNPs exposure causes oxidative stress-mediated JAK2/STAT3 signaling pathway activation thus to elicit pulmonary and systemic inflammation in the 45 days observation period in vivo, including of the elevation of TNF-α, IL-1β, and IL-6 levels in lungs and serum. The chronic inflammatory process activates TGF-Iβ/Smad3 signaling pathway so as to promote the transdifferentiation from fibroblast into myofibroblast, and finally accelerates the collagen production in lungs. However, the epithelial–mesenchymal transition in type II alveolar epithelial cells seems not involved in the process mentioned earlier.

consideration in intravenous exposure of nanomaterials in the biomedical application.

Oxidative stress is considered as one of the most important toxic mechanisms of nanomaterials including SiNPs.[8,22] With silicon-bonded hydroxyl groups and the unsaturated bond on the particle surface, SiNPs are prone to contribute to the generation of reactive oxygen species (ROS) and oxidative stress.[2] It was reported that SiNPs induced oxidative stress in a dose-dependent manner in vitro.[23–25] In present study, we observed SiNPs significantly increased oxidative stress markers MDA, depletion of SOD and GSH-Px in lung tissues through intravenous administration (Figure 2A). Oxidative stress mediated inappropriate activation of JAK2 and then activated the transcription factors STAT3 whose aberrant activation has been implicated in inflammation and carcinogenesis.[26,27] We detected the protein expression of JAK2/STAT3 signaling pathway and the results indicated SiNPs induced the activation of JAK2/STAT3 pathway (Figure 2B). Meanwhile, SiNPs elicited systemic inflammation and pulmonary inflammation illustrated by the elevation of TNF-α, IL-1β, and IL-6 levels in serum and lung tissues in mice (Figure 2C). Recently, Juthika Kundua et al also reported that SiNPs induced inflammation through JAK2/STAT3 pathway activation mediated by oxidative stress in human keratinocyte (HaCat) cells.[28] So our study demonstrated that the intravenous administration of SiNPs could elicit oxidative stress mediating JAK2/STAT3 pathway activation thus to cause pulmonary and systemic inflammation in the 45 days observation period in vivo.

During the tissue repair and wound healing, fibroblasts are promoted to transdifferentiate into myofibroblasts which are characterized by the de novo expression of αSMA and mainly in charge of production of extracellular matrix components including collagen, fibronectin, and others.[29] In our study, we demonstrated that intravenous injection of SiNPs induced moderate increase of αSMA expression and collagen accumulation in lung tissues in

the 45 days observation period (Figure 3A and C), indicating that SiNPs was likely to promote the transdifferentiation from fibroblast into myofibroblast thus to accelerate the production of extracellular matrix in lungs. Chronic inflammatory process is involved in the dysregulation of pulmonary fibroblast proliferation and contributes to overproduction of extracellular matrix.[30] Recently, it was reported that STAT3 mediated TGF-β production through the modulation of pro-inflammatory cytokines of IL-6 in pulmonary fibrosis.[31] We observed the upregulated protein expression of TGF-β and p-Smad3 in lungs in the SiNP-treated mice (Figure 3D). So in our study, the elevated protein expression of STAT3 and IL-6 contributed to the TGF-β production which promoted the transdifferentiation from fibroblast into myofibroblast so as to accelerate the collagen production in lungs.[29]

Generally, the origins of myofibroblasts are considered from interstitial fibroblasts through transdifferentiation, or from bone-marrow-derived fibrocytes in the blood circulation, or the alveolar epithelial cells type Ⅱ via EMT.[32,33] In our study, we observed SiNPs induced the ultrastructural changes in alveolar epithelial cells type II in lungs, but the protein expression of epithelial marker E-cadherin was elevated rather than reduced (Figure 4), which implied that most of the myofibroblasts involved in the excessive pulmonary extracellular matrix production did not originate from the transition of alveolar epithelial cells type Ⅱ in SiNP-treated mice. Hinz et al reported that myofibroblasts primarily generated from the transdifferentiation of the resident fibroblasts at the injury sites.[34] Yet, the underlying mechanism of the above issue required more investigation.

In summary, we found that SiNPs caused pulmonary inflammation and collagen accumulation through repeated intravenous injection in mice models. Furthermore, we revealed that oxidative stress and inflammation contributed to the collagen production through activation of JAK2/STAT3 and TGF-β/Smad3 signaling pathways, which is rare to see in previous toxicological researches on the lung tissues through repeated intravenous administration of SiNPs. It suggests that aberrant inflammation and collagen accumulation in lung tissues induced by nanoparticles should be seriously considered for the safety application in diagnostics or therapeutics, especially in the intravenous administration.

Acknowledgments

This work was supported by National Natural Science Foundation of China (No.81602876 and 81571130090), Support Project of High-level Teachers in Beijing Municipal Universities in the Period of 13th Five–year Plan (CIT&TCD201804089), and the Key Laboratory of Biomedical Effects of Nanomaterials and Nanosafety, CAS (NSKF201817).

Disclosure

The authors declare they have no conflicts of interest in this work.

References

1. Nel AE, Parak WJ, Chan WC, et al. Where are we heading in nanotechnology environmental health and safety and materials characterization? *ACS Nano*. 2015;9(6):5627–5630. doi:10.1021/acsnano.5b03496
2. Napierska D, Thomassen LC, Lison D, Martens JA, Hoet PH. The nanosilica hazard: another variable entity. *Part Fibre Toxicol*. 2010;7(1):39. doi:10.1186/1743-8977-7-39
3. Oberdorster G. Safety assessment for nanotechnology and nanomedicine: concepts of nanotoxicology. *J Intern Med*. 2010;267(1):89–105. doi:10.1111/j.1365-2796.2009.02187.x
4. Tang L, Cheng J. Nonporous silica nanoparticles for nanomedicine application. *Nano Today*. 2013;8(3):290–312. doi:10.1016/j.nantod.2013.04.007
5. WHO. *WHO Guidelines On Protecting Workers From Potential Risks Of Manufactured Nanomaterials*. Geneva: World Health Organization; 2017.
6. Xu R, Zhang G, Mai J, et al. An injectable nanoparticle generator enhances delivery of cancer therapeutics. *Nat Biotechnol*. 2016;34(4):414–418. doi:10.1038/nbt.3506
7. Benezra M, Penate-Medina O, Zanzonico PB, et al. Multimodal silica nanoparticles are effective cancer-targeted probes in a model of human melanoma. *J Clin Invest*. 2011;121(7):2768–2780. doi:10.1172/JCI45600
8. Murugadoss S, Lison D, Godderis L, et al. Toxicology of silica nanoparticles: an update. *Arch Toxicol*. 2017;91(9):2967–3010. doi:10.1007/s00204-017-1993-y
9. Yu Y, Duan J, Li Y, et al. Silica nanoparticles induce liver fibrosis via TGF-beta1/Smad3 pathway in ICR mice. *Int J Nanomedicine*. 2017;12:6045–6057. doi:10.2147/IJN.S132304
10. Yu Y, Li Y, Wang W, et al. Acute toxicity of amorphous silica nanoparticles in intravenously exposed ICR mice. *PLoS One*. 2013;8(4):e61346. doi:10.1371/journal.pone.0061346
11. Xie G, Sun J, Zhong G, Shi L, Zhang D. Biodistribution and toxicity of intravenously administered silica nanoparticles in mice. *Arch Toxicol*. 2010;84(3):183–190. doi:10.1007/s00204-009-0488-x
12. Zhuravskii S, Yukina G, Kulikova O, et al. Mast cell accumulation precedes tissue fibrosis induced by intravenously administered amorphous silica nanoparticles. *Toxicol Mech Methods*. 2016;26(4):260–269. doi:10.3109/15376516.2016.1169341
13. Mohammadpour R, Yazdimamaghani M, Cheney DL, Jedrzkiewicz J, Ghandehari H. Subchronic toxicity of silica nanoparticles as a function of size and porosity. *J Control Release*. 2019;304:216–232. doi:10.1016/j.jconrel.2019.04.041
14. Iwaisako K, Hatano E, Taura K, et al. Loss of Sept4 exacerbates liver fibrosis through the dysregulation of hepatic stellate cells. *J Hepatol*. 2008;49(5):768–778. doi:10.1016/j.jhep.2008.05.026
15. Morris AS, Adamcakova-Dodd A, Lehman SE, et al. Amine modification of nonporous silica nanoparticles reduces inflammatory response following intratracheal instillation in murine lungs. *Toxicol Lett*. 2016;241:207–215. doi:10.1016/j.toxlet.2015.11.006
16. Maser E, Schulz M, Sauer UG, et al. In vitro and in vivo genotoxicity investigations of differently sized amorphous SiO2 nanomaterials. *Mutat Res Genet Toxicol Environ Mutagen*. 2015;794:57–74. doi:10.1016/j.mrgentox.2015.10.005

17. Zhang J, Ren L, Zou Y, et al. Silica nanoparticles induce start inhibition of meiosis and cell cycle arrest via down-regulating meiotic relevant factors. *Toxicol Res (Camb)*. 2016;5(5):1453–1464. doi:10.1039/c6tx00236f
18. Yang H, Wu QY, Li MY, Lao CS, Zhang YJ. Pulmonary toxicity in rats caused by exposure to intratracheal instillation of SiO2 nanoparticles. *Biomed Environ Sci*. 2017;30(4):264–279. doi:10.3967/bes2017.036
19. Yang M, Jing L, Wang J, et al. Macrophages participate in local and systemic inflammation induced by amorphous silica nanoparticles through intratracheal instillation. *Int J Nanomedicine*. 2016;11:6217–6228. doi:10.2147/IJN.S116492
20. Choi M, Cho W-S, Han BS, et al. Transient pulmonary fibrogenic effect induced by intratracheal instillation of ultrafine amorphous silica in A/J mice. *Toxicol Lett*. 2008;182(1–3):97–101. doi:10.1016/j.toxlet.2008.08.019
21. Ferri C, Artoni E, Sighinolfi GL, et al. High serum levels of silica nanoparticles in systemic sclerosis patients with occupational exposure: possible pathogenetic role in disease phenotypes. *Semin Arthritis Rheum*. 2018. doi:10.1016/j.semarthrit.2018.06.009
22. Wang F, Gao F, Lan M, Yuan H, Huang Y, Liu J. Oxidative stress contributes to silica nanoparticle-induced cytotoxicity in human embryonic kidney cells. *Toxicol In Vitro*. 2009;23(5):808–815. doi:10.1016/j.tiv.2009.04.009
23. Sun L, Li Y, Liu X, et al. Cytotoxicity and mitochondrial damage caused by silica nanoparticles. *Toxicol In Vitro*. 2011;25(8):1619–1629. doi:10.1016/j.tiv.2011.06.012
24. Osmond-McLeod MJ, Poland CA, Murphy F, et al. Durability and inflammogenic impact of carbon nanotubes compared with asbestos fibres. *Part Fibre Toxicol*. 2011;8:15. doi:10.1186/1743-8977-8-15
25. Duan J, Yu Y, Yu Y, et al. Silica nanoparticles induce autophagy and endothelial dysfunction via the PI3K/Akt/mTOR signaling pathway. *Int J Nanomedicine*. 2014;9:5131–5141. doi:10.2147/IJN.S71074
26. Momtaz S, Niaz K, Maqbool F, Abdollahi M, Rastrelli L, Nabavi SM. STAT3 targeting by polyphenols: novel therapeutic strategy for melanoma. *Biofactors*. 2017;43(3):347–370. doi:10.1002/biof.1345
27. Kundu JK, Surh Y.J. Emerging avenues linking inflammation and cancer. *Free Radic Biol Med*. 2012;52(9):2013–2037. doi:10.1016/j.freeradbiomed.2012.02.035
28. Kundu J, Kim D-H, Chae IG, et al. Silicon dioxide nanoparticles induce COX-2 expression through activation of STAT3 signaling pathway in HaCaT cells. *Toxicol In Vitro*. 2018;52:235–242. doi:10.1016/j.tiv.2018.06.008
29. Razdan N, Vasilopoulos T, Herbig U. Telomere dysfunction promotes transdifferentiation of human fibroblasts into myofibroblasts. *Aging Cell*. 2018;e12838. doi:10.1111/acel.12838
30. Kolb M. Inflammation and dysregulated fibroblast proliferation–new mechanisms? *Sarcoidosis Vasc Diffuse Lung Dis*. 2013;30 (Suppl 1):21–26.
31. Celada LJ, Kropski JA, Herazo-Maya JD, et al. PD-1 up-regulation on CD4(+) T cells promotes pulmonary fibrosis through STAT3-mediated IL-17A and TGF-beta1 production. *Sci Transl Med*. 2018;10(460):eaar8356. doi:10.1126/scitranslmed.aao4496
32. Kim KK, Kugler MC, Wolters PJ, et al. Alveolar epithelial cell mesenchymal transition develops in vivo during pulmonary fibrosis and is regulated by the extracellular matrix. *Proc Natl Acad Sci U S A*. 2006;103(35):13180–13185. doi:10.1073/pnas.0605669103
33. Willis BC, duBois RM, Borok Z. Epithelial origin of myofibroblasts during fibrosis in the lung. *Proc Am Thorac Soc*. 2006;3(4):377–382. doi:10.1513/pats.200601-004TK
34. Hinz B. Formation and function of the myofibroblast during tissue repair. *J Invest Dermatol*. 2007;127(3):526–537. doi:10.1038/sj.jid.5700613